ELSEVIER

Field Crops Research 57 (1998) 209–222

Field Crops Research

A model of leaf area development and senescence for winter oilseed rape

B. Gabrielle [a,*], P. Denoroy [a], G. Gosse [a], E. Justes [b], M.N. Andersen [c]

[a] *Institut National de la Recherche Agronomique, Unité de Recherche en Bioclimatologie, Thiverval-Grignon, France*
[b] *Institut National de la Recherche Agronomique, Station d'Agronomie de Châlons-Reims, Reims, France*
[c] *Danish Institute of Plant and Soil Science, Department of Soil Science, Research Centre Foulum, Foulum, Denmark*

Received 25 February 1997; revised 22 October 1997; accepted 24 October 1997

Abstract

In winter crops, leaf area is a major determinant of the final yield, and is substantially affected by losses occurring during vegetative growth. Here, we propose and test a submodel simulating the development of leaf area and pod area, along with leaf senescence, for winter oilseed rape (*Brassica napus* L.), which was included in a CERES-type model for rape adapted from CERES-N Maize. This crop model, called CERES-Rape, has components for crop phenology, net photosynthesis, N uptake, and assimilate partitioning. As a new feature compared to previously published work, the leaf area submodel includes senescence from shading due to competition for light in the canopy, and from leaf N deficiencies. The model has been developed and parameterised on a 1-yr-long experiment with three fertilizer N treatments in northeastern France, during which measurements of senescing parts allowed calibration of the equations for leaf area index (LAI) senescence and total generated LAI. The leaf area submodel, once coupled to the CERES-Rape model, was tested against two additional experiments from Denmark and northern France. This process-oriented submodel proved accurate for the simulation of actual LAI whether in the calibration or in the validation phase, with an overall Root Mean Square Error (RMSE) of 0.496 m^2 m^{-2}, falling close to the mean experimental standard deviation. Extrapolation did not require any further adjustment, although a different cultivar was involved.

Keywords: Oilseed rape; Leaf area index; Soil–crop model; Process-oriented modelling

1. Introduction

Leaf area is a key factor for the interception of radiation and carbon assimilation by crops (Gosse et al., 1986; Sinclair, 1994). Therefore, the accurate modelling of the growth and development of crops in the field is conditioned by an adequate description of the dynamics of leaf growth and senescence, especially in the low range of crop leaf area index (LAI) to which intercepted radiation is most sensitive. In the particular case of autumn-sown crops, important losses of leaf area occur in winter due to freezing, and in spring due to senescence, which need to be taken into account for predicting the final yield. For winter rapeseed on which we focused here, Leterme (1985) observed a significant correlation between grain yield and green LAI at mid-flowering. The modelling of LAI losses and green LAI before the

* Corresponding author. IACR-Rothamsted, Harpenden, Herts, AL5 2JQ, UK. E-mail: benoit.gabrielle@bbsrc.ac.uk.

0378-4290/98/$19.00
PII S0378-4290(97)00147-0

onset of spring growth is then essential for determining crop yield. LAI losses also significantly affect the crop carbon and nitrogen budgets, and consequently the nitrogen losses from the soil–crop system.

Approaches to model crop LAI are either based on the gross leaf area of the canopy (Spitters et al., 1989; Petersen et al., 1995), or on the simulation of individual leaves growing on an average plant in this canopy (Sinclair and Amir, 1992; Soontornchainaksaeng et al., 1998; Villalobos et al., 1996), involving their appearance, development and senescence as related to competition effects for light, nutrient or water resources within the canopy. The former models use statistical regressions against thermal or calendar time (Petersen et al., 1995), or convert leaf dry matter (DM) into area through a fixed specific leaf weight (Spitters et al., 1989). They may include part of the above mentioned environmental stresses, reflecting, for instance, the small LAI associated with low soil N availability (Petersen et al., 1995), but they usually do not account for the net loss of leaf area occurring during the growth cycle that were of particular interest to us (Jensen et al., 1994; Gabrielle, 1996; Habekotté, 1996). On the other hand, models based on individual leaves often assume a fixed profile of maximum leaf area as a function of leaf number, and a fixed final number of leaves (Jones and Kiniry, 1986; Amir and Sinclair, 1991), which restricts their application to crops generating relatively few leaves, such as maize (*Zea mays* L.) or sunflower (*Helianthus annuus* L.). For rapeseed, in contrast, Mendham and Salisbury (1995) pointed out that the parameters of the leaf profile could vary according to genotype and latitude.

With the ultimate objective of assessing the yield and N losses of a winter rapeseed crop, using the CERES models (IBSNAT, 1990), we developed a simple submodel for its leaf area. Given the limitations underlined for both approaches to model the LAI of such a crop, we attempted to build a simple, mechanistic model including area losses due to lack of solar radiation or nitrogen during crop growth, without being based on the simulation of individual leaves. The model simulates on a daily basis (i) potential leaf area increase and (ii) leaf senescence. The rate of increase in area at the plant level is a function of Growing Degree Days (GDD), as modulated by leaf N concentration. Senescence then occurs (i) because of competition effects for solar radiation and N in the canopy and (ii) after flowering due to N translocation to grains and crop ontogeny. Losses induced by freezing were not dealt with, essentially because they had not been measured in the experiments, but their effect was generally marginal.

The equations of the submodel were sequentially calibrated on data of both total generated and green LAI obtained in a 1-yr-long experiment involving three fertiliser N treatments. A similar submodel was built for the simulation of crop Pod Area Index (PAI), though without taking senescence effects into account. These submodels were included in a global CERES-type model for crop growth and development, called CERES-Rape (Gabrielle et al., 1998), and tested on two independent data sets from Jyndevad, Denmark, and Grignon, France.

2. Materials and methods

2.1. Experimental data

In the model calibration and tests we used three data sets, which basic features are summarized in Table 1. The Châlons data set, including a monitoring of leaf senescence and death, was used for the calibration of the leaf and pod area relationships, whereas the Jyndevad and Grignon data sets served for testing the model predictions of actual LAI or PAI. Experimental details are given by Caron (1995) for Châlons and Grignon, and by Petersen et al. (1995) and Andersen et al. (1996) for Jyndevad.

In all experiments, crops were fully irrigated and weed- and pest-protected so that associated stresses were negligible. Daily climatic data (global radiation, minimum and maximum air temperatures, precipitation and potential evapotranspiration) were measured at a local weather station located within 1 km from the experimental fields.

In Châlons, three replicate 600-m^2 blocks arranged in a split-plot design with N treatment as main plot and sampling date as subplot were sown in 0.29-m rows in late summer. Every 2 or 3 weeks, in each block, three subsamples of 0.435 m^2 were collected, yielding a surface of 1.3 m^2 $replicate^{-1}$.

Table 1
Selected characteristics of the three experiments used for calibration and testing of the model

Name and location	Soil	N treatments		Cultivar	Sowing and harvest dates
		Name	Fertilizer N doses (g N m^{-2})		
Châlons 41.2N 6.7E	Rendzina over chalk	N0	0	Goéland	9/8/94
		N1	15.3		7/11/95
		N2	27.2		
Grignon 48.9N 1.95E	Silt loam	S1	3.3	Goéland	3/23/95[a]
		S2	3.3		4/6/95[a]
Jyndevad 54.3N 12.3E	Coarse sand	N0	4.8	Ceres	8/20/91
		N1	15.5		7/15/92
		N2	26.1		

[a] In Grignon, the two sowings were monitored only during the first 3 months, in the crop establishment phase.

In Jyndevad, three autumn-sown (0.12-m rows) N treatments were established in 15.2-m^2 plots arranged in a randomised block design, with four replicates. Samples of 0.5 m^2 were taken in each plot every 10 days in spring.

In Grignon, crops were sown in 0.28-m rows in spring, in a split-plot design with sowing date as main plots, and sampling date (three replicates, each 0.42 m^2) as subplots. Sampling was performed every 2 weeks until early summer, before flowering occurred. After emergence, plant densities amounted to ca. 60 plants m^{-2} in Châlons and Grignon, and remained fairly constant. Plant density was only counted after harvest in Jyndevad, when it amounted to 90 plants m^{-2}.

In all experiments, leaf samples were split into green and senescent fractions, and the surfaces were measured with an optical leaf area meter. Leaves were categorised as senescent if more than half of their surface appeared yellow. Leaves were then weighed after drying for 48 h at 80°C, and analysed for nitrogen (Dumas method) in order to calculate the specific leaf N (SLN, g N m^{-2}). Pods were sampled only in Châlons and Jyndevad, and analysed according to a similar procedure, although no senescent fraction was visible in Châlons.

In Châlons, prior to the onset of flowering and stem branching, the losses of leaf area and biomass were assessed by indirect measurements in the field. In each block, for a given sampling date, one of the three subsamples collected was used to determine the distribution of individual plant size according to base crown diameter, resulting in a stratification into six classes. The number of leaf scars at the base of the stems was also counted, as an indicator of both the number of leaves fallen since the last sampling date and the rank of appearance of present leaves. About 30 plants were then randomly sampled in the field, among which three representatives of each class were taken for a detailed analysis of their leaf area profile, in which individual leaves were characterised as a function of their ranks in terms of area and specific weight (SLW, g dry matter m^{-2}). The sample stratification allowed the estimation of the mean area profile for each plant class, and these profiles were further averaged across classes and blocks for each N treatment. Date-to-date comparison of these profiles yielded the losses of LAI as well as the total LAI generated.

After the onset of stem branching we hypothesised that no senescence occurred for the leaves growing on branches before flowering, i.e., the end of leaf growth. After that date, no new leaf area appeared so that the net decrease of LAI corresponded to senescent LAI.

Throughout the growing season, area losses were converted into biomass and N losses by using the SLW and SLN measured on the senescent leaves collected in the field at that time in the plots.

2.2. Model evaluation and sensitivity

The goodness of fit of the model was assessed on the basis of both visual comparisons between simulated and field-measured values, and quantitative

statistical measures, as recommended by Smith et al. (1996). The statistical criteria we used to compare the time series of mean modelled and actual LAI are the correlation coefficient (r), giving the association between the two series, and the Root Mean Square Error (RMSE). RMSE is here defined as: $\mathrm{RMSE} = [\Sigma(O_i - P_i)^2/n]^{1/2}$, where O_i and P_i are the observed and predicted values of LAI, respectively, and n is the number of sampling dates.

Because there were no literature values available for a small numbers of parameters relating to leaf senescence, these had to be visually fitted to the experimental data of the calibration set. The sensitivity of the model to individual variations in the parameters around their optimum values was then analysed by computing a RMSE for the simulated green LAI lumped over the three Châlons treatments. The parameters were varied one at a time within a relative range of $\pm 25\%$.

2.3. Modelling of leaf area

2.3.1. Potential LAI expansion rate

Before accounting for any senescence effect, the potential LAI expansion rate is modelled as a function of Growing Degree Days (°C), since it has been noted for various crops by authors such as Amir and Sinclair (1991), Morrison et al. (1992) and Soontornchainaksaeng et al. (1998) that new leaves emerge at fixed GDD intervals, and then expand at a fixed rate, although this rate is affected by leaf number. The rate of leaf area increase at the canopy level would then be a function of thermal time. Here, the daily increment in leaf area ($\Delta \mathrm{LAI}_{\mathrm{pot}}$) depends on current LAI and on daily growing degree days with a base temperature of 4.5°C, noted $\mathrm{GDD}_{4.5}$. The base temperature was adjusted on the Grignon data by Caron (1995), and is close to the value of 5°C cited by Morrison et al. (1992) for summer rapeseed in Canada.

Two stages are distinguished: the daily leaf expansion rate increases exponentially until cumulative $\mathrm{GDD}_{4.5}$ from emergence reaches 600, and afterwards becomes constant. Thus:

$$\Delta \mathrm{LAI}_{\mathrm{pot.}} = 7.89 \times 10^{-3} \mathrm{LAI}^{0.629} \mathrm{GDD}_{4.5} \quad \textit{if } \mathrm{LAI} \le 2.5$$
$$\Delta \mathrm{LAI}_{\mathrm{pot.}} = 0.038 \mathrm{GDD}_{4.5} \text{ otherwise.} \qquad (1)$$

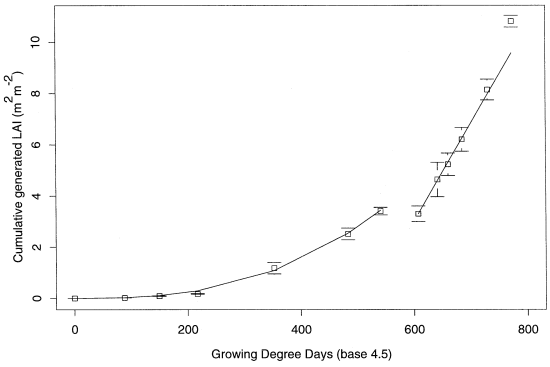

Fig. 1. Total generated LAI for the N2 crop in Châlons (symbols), as a function of thermal time. The solid line represents a exponential then linear regression on the Châlons data (RMSE = 0.42 m^2 m^{-2}, $n = 11$). The interval between the sixth and seventh sampling dates was rejected because of a severe freezing period that induced losses of green LAI, and causes a discontinuity in the regression lines.

The coefficients in Eq. (1) were deduced from multiple regression on the Châlons data for the N2 treatment (Fig. 1), considering that this treatment was neither water nor N limited at any time.

2.3.2. N stress on leaf expansion rate

In case of N deficiencies in the leaves, the potential rate $\Delta \mathrm{LAI}_{\mathrm{pot}}$ is multiplied by a dimensionless 0–1 factor calculated by the crop N uptake routine of CERES-Rape, corresponding to the crop N Nutrition Index (NNI). The NNI (see, e.g., Lemaire et al., 1989) is based on the existence of a critical N concentration in shoot tissues, at which crop utilisation of N is optimal as regards biomass production. This critical concentration, noted $\mathrm{N_c}$ (%, w/w), has been shown to decrease with increasing aerial biomass, with a relationship nearly identical for all $\mathrm{C_3}$ crops (Greenwood et al., 1990). We used a similar equation recently adjusted for rapeseed by Colnenne et al. (to be published in Annals of Botany, 1998), with:

$$\mathrm{N_c} = 4.48 \mathrm{DM}^{-0.25} \text{ if } \mathrm{DM} \ge 0.9$$
$$\mathrm{N_c} = 4.60 \text{ otherwise,} \qquad (2)$$

where DM is the shoot dry matter (t ha^{-1}). This critical N rigorously pertains to DM production, but proved a reasonable approximation to characterise

leaf expansion for herbage stands (Gastal et al., 1992).

Crop NNI then equals the ratio of actual to critical N content in aerial parts: $NNI = N_a/N_c$, where N_a is the actual N concentration. As suggested by Gastal et al. (1992) and Duru et al. (1995) for herbage stands, the potential, temperature-limited rate of LAI growth is multiplied by the NNI, with NNI being however bounded between nil and unity. This implies that the rate of leaf elongation does not respond positively to leaf N concentration above N_c, which is an approximation since such a saturation effect was observed only for NNI higher than 1.4 for tall fescue (*Festuca arundinacea*, L.) by Gastal et al. (1992).

2.3.3. Shading-induced senescence

Shading-induced leaf senescence occurs at the bottom of the canopy if the transmitted radiation drops beneath a given threshold (Derache and Guen, 1986; see Fig. 2). This threshold level of radiation corresponds to an equilibrium in the plant carbon budget where gross photosynthesis exactly compensates for losses by respiration. The attenuation of photosynthetically active radiation (PAR) within the canopy obeys Beer's Law, with: $PAR_t = PAR \exp[-kLAI]$. PAR_t (MJ m^{-2} day^{-1}) is the PAR transmitted beneath a layer of area index LAI, PAR is the incoming radiation, and k an extinction coefficient set to 0.75 for rapeseed, as derived from Gosse et al. (1983) and Andersen et al. (1996). By inverting the above equation, one can calculate the maximum LAI (LAI_x) that can be maintained for a given PAR, as:

$$LAI_x = 1/k \log\left[PAR/(PAR_x f_T)\right] \quad \text{if } PAR \geq PAR_x f_T \qquad (3)$$
$$LAI_x = 0 \text{ otherwise,}$$

where PAR_x corresponds to the threshold radiation required for maintenance respiration, below which the bottom layers of leaves start senescing. Since crop respiration is affected by temperature, PAR_x is multiplied by a temperature factor f_T involving an Arrhenius law with a Q_{10} of 2 and an optimum at 20°C. The resulting amount of senescent LAI (ΔLAI_S) thus reads:

$$\Delta LAI_S = LAI - LAI_x. \qquad (4)$$

However, to take into account a buffering capacity of plants against the loss of LAI, and to reduce mathematical instabilities due to the daily time step of the model, this senescence is equally split over 3 days, and so that if during that period solar radiation can maintain a higher LAI, the loss is accordingly diminished.

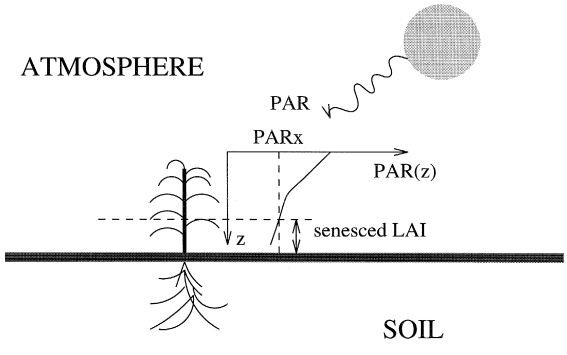

Fig. 2. Modelling of leaf senescence induced by shading. Senescence is induced in the bottom layers of leaves that receive a transmitted radiation less than the PAR_x threshold (see text).

2.3.4. Senescence from N deficiencies

Senescence also occurs in the vegetative phase because of N deficiency in leaf tissues, as observed in rapeseed by Triboi-Blondel (1988). In a lucerne canopy, Lemaire et al. (1991) found a close relationship between the vertical distributions of light and specific leaf N (SLN, g N m^{-2}), with an abrupt decrease of SLN beneath the layer of leaves receiving less than 15% of the incoming radiation. They hypothesised that during their growth cycle, leaves were gradually shaded by newly generated leaves, and supplied N to these new leaves until their specific N dropped below a threshold value, here noted MSLN (Minimum SLN), which marked the onset of senescence and abscission. After leaf fall, Lemaire et al. (1991) found that SLN had dropped to a value smaller than MSLN, denoted SSLN (Structural SLN), which they suggested corresponded to a structural fraction, whereas the N mobilized during senescence (and leading from MSLN to SSLN) constituted a metabolic fraction. We thus assumed, at the canopy level, the existence of a minimum specific leaf N content (MSLN, g N m^{-2}), under which a fraction of leaf area becomes senescent, with a SLN corresponding to the structural concentration (SSLN, g N

m^{-2}). The amount of senescent LAI due to N deficiency, noted ΔLAI_N, is calculated as:

$$\Delta LAI_N = LAI \frac{MSLN - SLN}{MSLN - SSLN}, \quad (5)$$

where SLN is the actual specific leaf N (g N m^{-2}). Eq. (5) applies only if $SLN \leq MSLN$, otherwise ΔLAI_N is nil.

In the reproductive phase, LAI peaks around mid-flowering, after which translocations of N from leaves to pods occurs until crop maturation (Andersen et al., 1996). In the model, a pool of N available from stems and leaves is calculated at mid-flowering, from which date the daily translocation flux of N to the pods is proportional to daily Growing Degree Days (base 0°C). The loss of leaf area resulting from this loss of N from the leaves is calculated as:

$$LAI_N = LTRN/(SLN - SSLN), \quad (6)$$

where LTRN is the translocation flux from the leaves (g N m^{-2} day^{-1}).

After all senescent fractions have been computed, the daily change in LAI is calculated as: $\Delta LAI = \Delta LAI_{pot.} \times NNI - \Delta LAI_C - \Delta LAI_N$.

2.3.5. Leaf C and N budget

In the CERES-Rape model, daily crop dry matter (DM) accumulation is calculated from intercepted photosynthetically active radiation (PAR_i) assuming a constant radiation-use efficiency of 2.4 g DM MJ^{-1} PAR_i (Gosse et al., 1983; Andersen et al., 1996) for vegetative parts, which is also modulated by leaf N (Gabrielle et al., 1998). Incoming PAR is taken to represent 50% of global radiation (Varlet-Grancher et al., 1982). Newly generated leaves have a specific leaf weight (SLW, g DM m^{-2}) that depends on leaf number (lnb), with (Caron, 1995):

$$\begin{aligned} &SLW = 60 \text{ for } lnb \leq 14 \\ &SLW = 60 + 30/7(lnb - 13) \text{ for } 14 < lnb \leq 20 \\ &SLW = 90 - 30/12(lnb - 20) \text{ for } lnb > 20 \end{aligned} \quad (7)$$

To determine lnb, a thermochrone of 75 GDD_1 (base temperature of 1°C) is assumed (Mendham and Salisbury, 1995).

As in CERES-Maize, the daily demand for N of the aerial vegetative compartments (stems and leaves) is a linear function of the difference between their N concentration and the critical concentration N_c given in Eq. (2). This demand may not be met if the N supply from soil, as calculated in the crop N uptake routine, is limited. For senescing leaves, a SLW of 20 g m^{-2} is assumed, based mainly on model calibration for the simulation of leaf dry matter (Gabrielle, 1996). This value is indeed quite low compared to the 40–60 g m^{-2} range obtained from measurements on dead material collected in the field on plastic grids within 1 week after leaf fall. However, this SLW was found to be relatively insensitive (Table 2). The specific leaf N of dead leaves was set to the structural content SSLN, which value was calibrated at 0.5 g N m^{-2}. As with SLW, the latter value was also significantly smaller than the range of 0.8–1.2 g N m^{-2} measured on dead material. However, using a corresponding median value of 1.0 g N m^{-2} resulted in a systematic overestimation of leaf N losses by the model. In addition, the area of the dead leaves collected is likely to have been underestimated because leaves had started to decompose,

Table 2
Percentage variations of model error (RMSE) as a result of variations in the parameters relating to leaf senescence for the Châlons treatments (Parameter variations are expressed in percentage relative to their baseline value, and the RMSE in percentage relative to a baseline value of 0.559 m^2 m^{-2})

Parameter and unit	Baseline value	−25%	−10%	+10%	+25%
		RMSE (m^2 m^{-2})			
Specific leaf nitrogen of dead leaves (g N m^{-2})	0.5	8.72	3.50	−3.05	−6.73
Specific leaf weight of dead leaves (g DM m^{-2})	20.0	0.62	0.18	−0.18	−0.36
Threshold radiation (PAR_x) (MJ PAR m^{-2} day^{-1})	0.4	6.63	1.70	−1.18	−2.23
Minimum specific leaf nitrogen (MSLN)					
Upper boundary (g N m^{-2})	2.3	93.42	26.02	−7.72	−10.21
Power coefficient (unitless)	−0.5	−4.50	−2.18	2.50	7.01

leading to an overestimation of the dead leaf SLW and SLN.

2.3.6. Pod area growth

In the model, pod growth starts after the day of mid-flowering, and pod area expands during a fixed time interval of 250 $GDD_{4.5}$, corresponding to the mean duration observed in Châlons. Daily increase in Pod Area Index (PAI, $m^2\ m^{-2}$) is then proportional to daily $GDD_{4.5}$, with PAI being bounded by a fixed maximum potential noted PAI_{max}. This potential rate is diminished if available N is not sufficient in the pod walls, with the stress factor similar to the NNI used for leaf growth, although there is strictly no theoretical basis to the concept of a critical N content in the pod compartment. To compute the N stress factor, we derived a purely empirical 'critical' curve for the N concentration in the pod walls, using the N2 data in Châlons as a non N-limited reference (Gabrielle, 1996). The daily PAI increase, ΔPAI, is then given by the following equation:

$$\Delta PAI = GDD_{4.5}/250 PAI_{max} N f_{pw}, \quad (8)$$

where Nf_{pw} is the ratio of actual to 'critical' N concentration in the pod walls. PAI_{max} was set to 2.5, which corresponded to observations for the N2 treatment in Châlons used for calibration.

After the expansion period, the PAI decrease induced by pod senescence is not simulated.

3. Results and discussion

3.1. Model calibration

In this stage, the parameters of the various equations of the model were calibrated, using only the Châlons data for internal consistency.

The adequacy of the modelling of N stress on leaf elongation was first checked by simulating the total LAI generated for the low N treatments (N0 and N1) in Châlons (Fig. 3). These results were from the global CERES-Rape model, in which Eqs. (1) and (2) for potential and N limited leaf expansion were introduced. The crop carbon and N budgets, as given by CERES-Rape, were necessary for computing the NNI factor. The soil and crop components of the model, except for the leaf area submodel that was of interest here, had previously been calibrated by Gabrielle (1996).

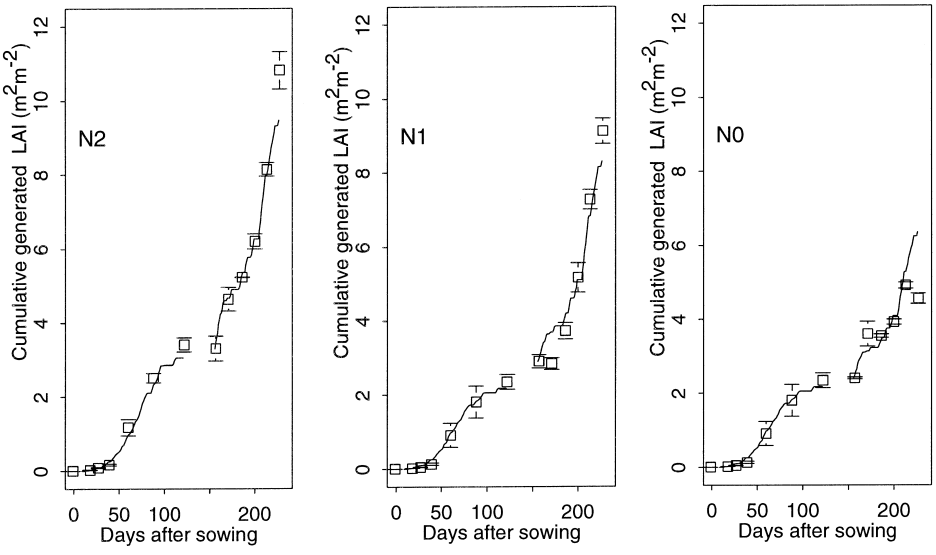

Fig. 3. Simulated (lines) and observed (symbols, ±s.d.) total generated LAI using the CERES-Rape model, for the three N treatments of Châlons, after calibration of the potential leaf expansion rate on the N_2 data. Due to the freeze event, the model was reinitialised on day after sowing 160.

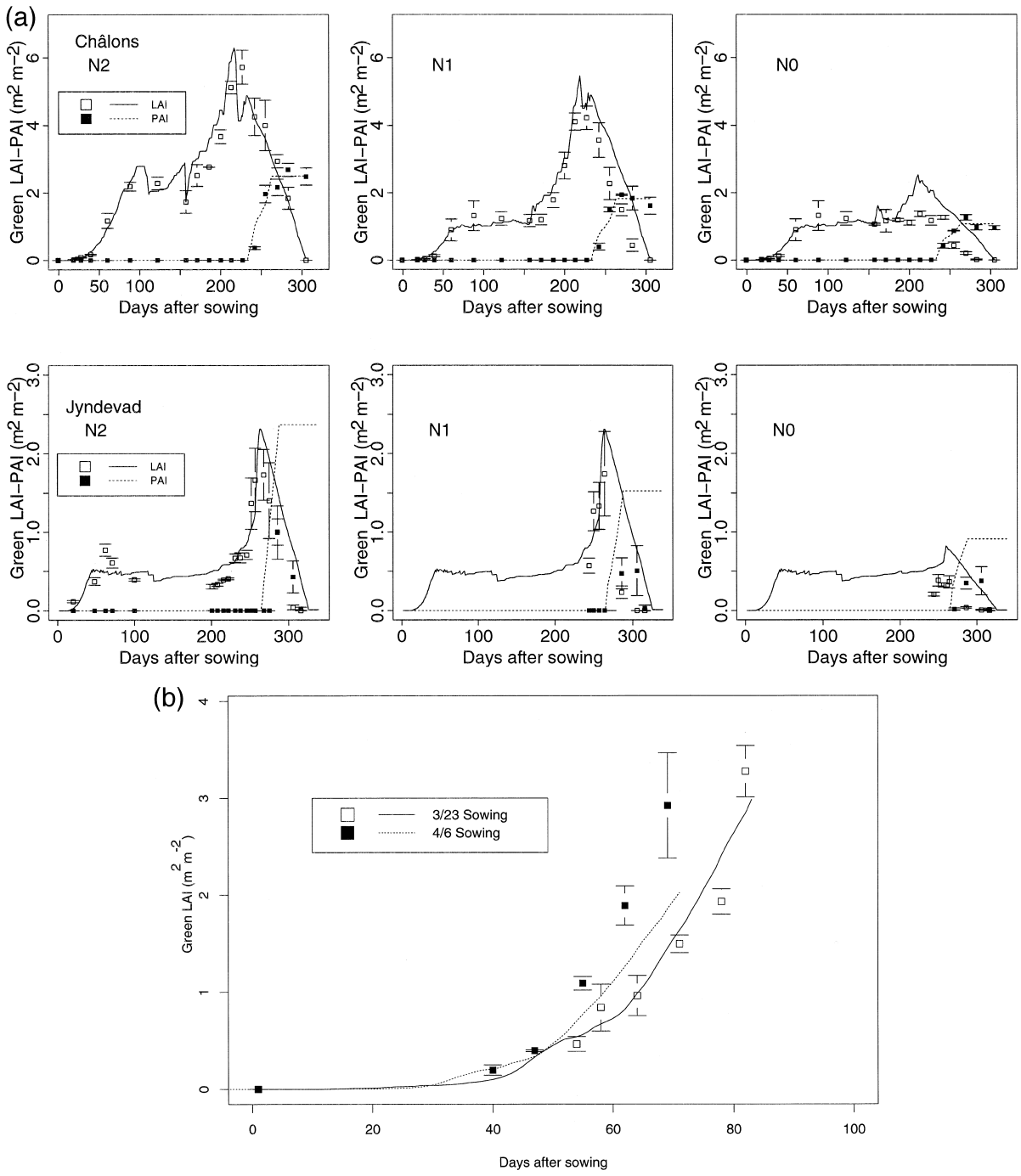

Fig. 4. Simulated (lines) and observed (symbols, ±s.d.) green LAI and PAI using the CERES-Rape model: (a) for the three N treatments of Châlons and Jyndevad, after calibration of the equation for senescence from inadequate leaf N content on the Châlons data, (b) for the two sowing dates in Grignon (LAI only).

The agreement between simulated and measured values of total generated LAI on Fig. 3 was good, although the simulated values had to be reinitialised after the freezing period (in early January), because of leaf area loss due to freezing that could not be accounted for by the model. The reinitialisation concerned the green LAI as well as leaf DM and N content. The fit was best in the autumn, after which discrepancies appeared for both N1 and N0 treatments. They may partly be ascribed to experimental uncertainties, as noticeable from the contradictory simulations of the total LAI data immediately after the freeze: the LAI was constant for the N1 treatment, against a 0.5 m^2 m^{-2} increase for the N0 crop, which is opposite to the expected trends. At the end of the period described in Fig. 3, total LAI reached a plateau because it corresponded to the date of flowering after which no new leaves appeared and translocation of N from vegetative parts induced a progressive senescence of existing leaves. Simulated total LAI was then underestimated for the N1 and N2 crops, and overestimated for the N0 crop. For the former case, it could be expected since a similar trend appeared in the regression of total LAI against $GDD_{4.5}$ on Fig. 1. The apparent change in the rate of increase in LAI at the end of the regression period might result from stem branching inducing a faster generation of leaves, or from an inaccurate determination of the base temperature. As regards to the N0 crop, it seems that the NNI factor calculated to model the N stress on leaf elongation was not drastic enough for the low ranges of leaf N. Actually, the zero LAI growth observed at the right-hand side of Fig. 3 for N0 could only have been reproduced by a NNI of zero, which is inconsistent with the hypothesis of a structural N content in the leaves. This has prompted some authors (e.g., Jones and Kiniry, 1986) to introduce such a minimal content in the N stress factor, allowing zero-responses.

Eq. (3) for shading-induced senescence was then calibrated against data of actual LAI for the N2 treatment (Fig. 4). It gave a value for PAR_x of 0.2 MJ m^{-2} PAR day^{-1}, which was assumed valid regardless of crop N status. This value may be compared to the maintenance respiration of the bottom layer of leaves receiving this level of radiation. By assuming a mean SLW of 70 g DM m^{-2}, and using the respiration costs and gross photosynthesis efficiencies given by Petersen et al. (1995), the product PAR_x times f_T in Eq. (3) is found to correspond to the maintenance requirements of 1.5 units of LAI, whatever the temperature.

After the freeze, the effects of which are clearly noticeable on the observations around day after sowing (DAS) 150, the simulated green LAI tended to be too high, despite the reinitialisation. On the other hand, immediately before the freeze, the model predicted heavy LAI losses for the N2 crop that did not seem to occur, when compared to the two corresponding measurements (DAS 100–140), or may have occurred later. Such a discrepancy also occurs for all treatments around the LAI peak at flowering, and could not be avoided in the calibration. Since these trends were not noted for the total LAI generated, it underlines a weakness of the empirical approach to shading-induced senescence undertaken here. It may also imply that the arbitrary buffering period of 3 days should last longer.

Finally, the simulation of senescence from insufficient N in leaves was adjusted by calibrating the MSLN parameter (Minimum Specific Leaf N; see the end of the Model description section), so as to fit to the actual observed values of LAI (Fig. 4).

MSLN was made dependent on green LAI because senescence appeared relatively less marked for well-developed canopies. This is illustrated on Fig. 5, where for all treatments the measured specific leaf N contents were in the same range, only medium values associated with low LAI hindered net LAI growth. This is noticeable on the data points for the N0 treatment, which are clustered in the region corresponding to LAI of 1–1.3 and SLN of 2–3 g N m^{-2}. In contrast, the N1 leaves were able to accumulate DM and expand as soon as their SLN rose to 4 g N m^{-2} after they received some fertiliser N in early spring. The solid line representing MSLN on Fig. 5 may be viewed as a lower boundary for the data points, but it was essentially deduced by model adjustment. It is however interesting to note that it was also close to the data corresponding to senescent leaves (Fig. 5). The upper boundary value of MSLN proved to be a very sensitive parameter, with a relative decrease of 10% entailing a 26% rise in model error (Table 2). Table 2 also revealed an optimum value of $\approx$ 2.75 g N m^{-2} for this parameter. However, using this value led to a significant

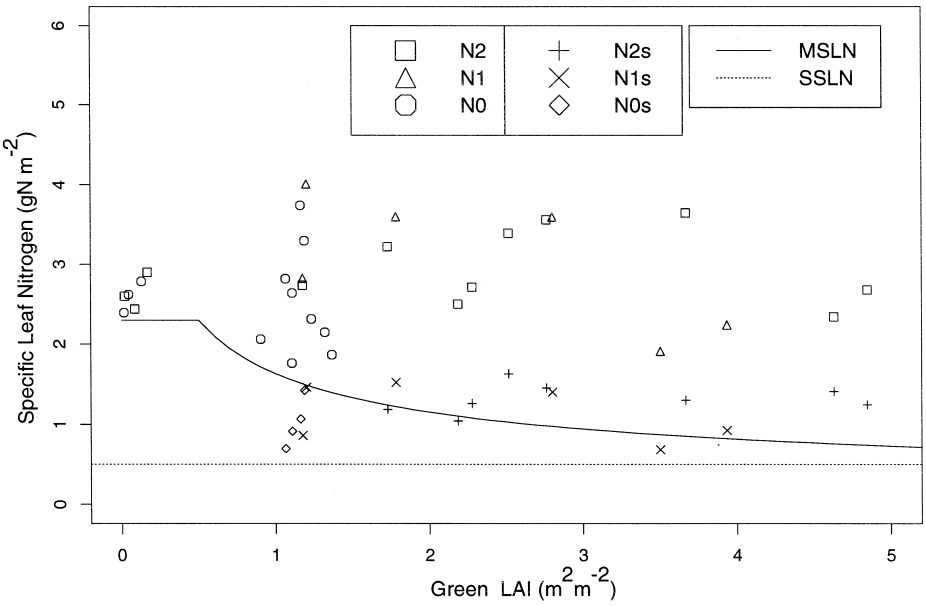

Fig. 5. Specific leaf N contents (g N m^{-2}) observed for the three N treatments in Châlons, as a function of green LAI. The data for the senescent leaves are marked with an 's' suffix. The solid line represents the minimum concentration under which senescence occurs (MSLN), and the dashed line is the concentration in the dead leaves (SSLN).

underestimation of LAI throughout autumn and winter, which was inconsistent with the fact that the model should have been rather overestimating LAI because it did not account for the freeze. The optimum was then rejected. Conversely, the power coefficient in Eq. (9) was little sensitive. MSLN (g N m^{-2}) was thus calculated as:

$$\begin{aligned} &\text{MSLN} = 1.81\text{LAI}^{-0.5} \text{ if LAI} \geq 0.5 \\ &\text{MSLN} = 2.3 \text{ otherwise.} \end{aligned} \quad (9)$$

The only calibration in Eq. (8) for PAI development consisted in setting the maximum potential PAI value (PAI_{max}) at 2.5, as observed in Châlons. It is however worth noting that for the N2 treatment the dynamics of PAI were also correct, although it only concerned four data points. The simulated final PAI was slightly overestimated for the other treatments, which should be ascribed to a bias in the N stress factor ($\text{N}f_{\text{pw}}$ in Eq. (8)), that must have been too high. However, the N content of pod walls was underpredicted by the model (up to 30%), implying that the stress factor curve should be a convex rather than linear function of $\text{N}f_{\text{pw}}$. The critical N equation employed might also be unfit to pod development, because there were only little data available in Châlons for estimating this curve.

3.2. Model testing

The Châlons data on Fig. 4 provided a first test of the leaf area submodel. For all treatments, the agreement was highly significant, with Root Mean Square Error (RMSE) in the range 0.52–0.61 m^2 m^{-2} and correlation coefficient (r) ranging from 0.82 to 0.95 (Table 3). The RMSE was somewhat high due to the overprediction by the model after DAS 150 which was previously noted in the calibration phase for the N2 treatment, and also appeared for the other treatments. This trend was smoothed later in the season, although for the unfertilised crop a second LAI peak was simulated in spring that did not match observations. In addition, the simulated decline of LAI after flowering was too slow. From DAS 160 to DAS 210, leaf senescence seems to have been underestimated by the model, yielding values of green LAI higher than observed. In addition to the discrepancies pertaining to shading-induced senescence, it may also involve the simulation of senescence from N for the

Table 3
Root mean square errors (RMSE) and correlation coefficients (r) for the simulations of green LAI by the CERES-Rape model

Location and treatment	RMSE ($m^2\ m^{-2}$)	r	n[a]
Châlons			
N2	0.539	0.954	16
N1	0.613	0.955	16
N0	0.521	0.820	16
Jyndevad			
NN2	0.301	0.878	19
N1	0.621	0.761	8
N0	0.326	0.862	7
Grignon			
S1	0.239	0.982	5
S2	0.572	1.000	5

[a] Number of observations.

N-limited treatments. However, the simulated specific leaf N data were actually also too low throughout that period (Fig. 6). For all treatments, a marked increase of the N concentration in leaf tissues was observed at that time, despite increasing biomass, which effects could not be explained by the concept of critical N content utilized by the model. This point emphasises the coupling of leaf area, C and N budgets, which impeded an accurate simulation of leaves because of persistent biases in the rest of the crop carbon and N routines (Gabrielle et al., 1998). For instance, the N content of dead leaves was a sensitive parameter, for it interacted with green leaf N content and subsequent leaf area losses. Lastly, the LAI decrease observed after flowering was faster for the N-limited treatments, which resulted in the model overestimating LAI at the end of the growth cycle. The sink effect of the pods for translocated N from the leaves must then have been stronger for the N0 and N1 crops than for the N2 crop. This should be accounted for, but has little influence since leaf photosynthesis is not significant for crop yield at that time.

The experimental fit of the Jyndevad and Grignon simulations in Fig. 4 was satisfactory although not as good as for Châlons, with RMSE in the range 0.30–0.62 $m^2\ m^{-2}$ in Jyndevad, and 0.24–0.57 in Grignon, and r coefficients in the range 0.76–1.00 overall (Table 3). Model parameters were identical to those established for Châlons, except for the date of flowering in Jyndevad, which was set at its experimental value. In Jyndevad, the rate of LAI decrease after mid-flowering predicted by the model was too slow, especially for the N0 and N1 treatments. This trend appeared more marked than in Châlons where it had already been noted. The model also tended to overestimate LAI before regrowth in spring, a trend which persisted for the N0 treatment throughout the rest of the season. For the other treatments, the LAI development rate was rather underestimated during spring regrowth.

Differences among cultivars with regard to leaf elongation rates and specific leaf weight have been reported for rape (Mendham and Salisbury, 1995), and may explain why the LAI development rates inferred in Châlons for cv. Goéland could not be readily applied to cv. Ceres used in Jyndevad. However, this approximation seemed of relatively low impact since it did not result in major discrepancies. Another factor likely to account for the biases in the Jyndevad simulations could be a lower base tempera-

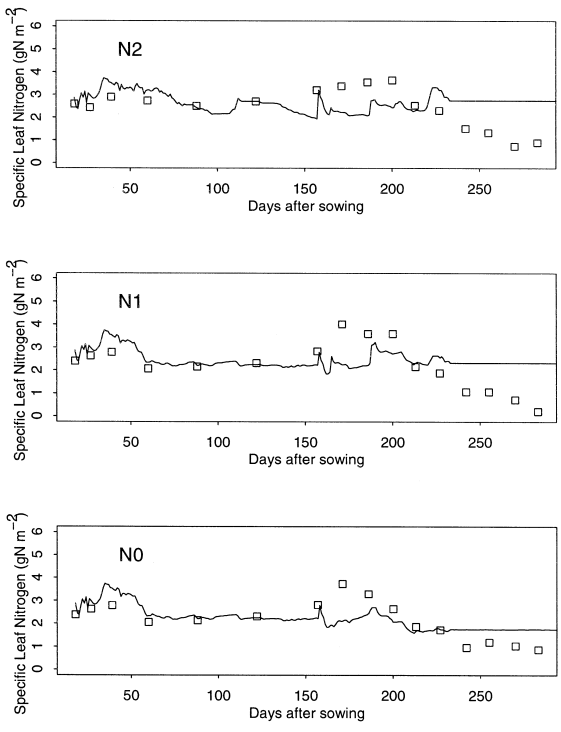

Fig. 6. Simulated (lines) and observed (symbols) Specific Leaf N contents (g N m^{-2}) for the three N treatments in Châlons, as a function of time.

ture for Ceres. For various Canadian spring cultivars grown in autumn, Hodgson et al. (1978, cited by Mendham and Salisbury, 1995) reported values ranging from 0 to 6°C. Apparent base temperatures may also vary with the levels of radiation to which the crop is subjected, for instance because of differences between apical and air temperatures. For a spring-sown maize crop in France, Cellier et al. (1993) measured values of apex temperatures between 0 and 6°C higher than air temperatures in the daytime. Such an effect could explain why the Grignon sown-spring crop seemed to present a lower base temperature than the autumn-sown crop of Châlons (same cultivar), given that it also appeared that leaf area was generated faster in Grignon than in Châlons (Caron, 1995). It was also pointed out by Sinclair (1994) that the base temperature depends on the temperature range on which it was obtained, with this range being higher in Grignon than in Châlons. This argument may also account for the underprediction of leaf expansion rates in Jyndevad, where temperatures were substantially lower than in Châlons (i.e., the true base temperature would be lower than 4.5°C in Jyndevad).

The basic problem with the model validation in Jyndevad and Grignon is that errors in the simulation of leaf senescence or leaf expansion rate could compensate and result in a good fit against actual LAI data. The results on Fig. 4 should then be regarded as a partial test, on the basis of which the goodness of the individual equations of the model and their parameters may not be fully discussed. Monitoring of leaf senescence should then be encouraged for a proper modelling of leaf area in winter crops.

However, multi-location tests of the model against data of actual LAI, if they reflect a sufficient variety of climatic conditions, may circumvent this feature of incompleteness, because a successful extrapolation cannot be in every case ascribed to compensations in model errors. In that respect, the tests in Jyndevad and Grignon indicate that the leaf area model could be successfully extrapolated to other conditions. Although no general conclusion may be drawn from these particular instances, they give support to further development and testing of the model. Because of its deterministic, process-based structure, this model may be expected to be valid for a range of pedo-climatic and cultivar conditions, as is the case for the mechanistic maize model of Muchow et al. (1990).

Finally, as regards PAI, the simulations in Jyndevad could not be compared to observed data because the latter represented only the green fraction, whereas the former did not include senescence effects. Qualitatively, it may however be concluded that the onset of PAI development was too early in the model, although the timing of the LAI peak was appropriate. It may then be that with the particular phenology of Ceres, a time lag of 1–2 weeks should be allowed between mid-flowering and the onset of pod elongation.

4. Conclusion

For the three locations tested, it appeared that the dynamics of leaf area expansion and senescence could be explained to a large extent by the equations we proposed and calibrated on the Châlons data set. The fine level of investigation associated with the latter allowed a precise, process-by-process analysis of leaf area development, which constituted a sound basis for modelling.

Because the collection of such detailed data is rather time-consuming, we expect that our model may usefully supplement field trials and help reconstruct the dynamics of LAI for rapeseed over a range of climatic and genotype conditions. In addition, its mechanistic features should make an accurate simulation of leaf area possible with the calibration of only a few parameters. Such seemed to be the case for the two independent data sets we used, involving another climate and another rape cultivar, and it provided favourable examples. In the Jyndevad test, it is interesting that the CERES-Rape model was able to predict LAI levels that were systematically lower than with the Châlons data set used for calibration, due to lower temperature levels and a shorter growing cycle.

There are still processes to be included in the model, such as leaf freezing and water stress, which may play an important role (Andersen et al., 1996). They could be implemented in the model and calibrated in the same way as for the equations for N stress and senescence from N deficiencies, provided that data covering a sufficient range of environmen-

tal conditions be available, along with field-estimations of leaf area losses. The last point is rather tedious and delicate, but appears essential.

Lastly, the leaf area model should be a fair basis for further testing of the CERES-Rape model. Those results are presented in a companion paper (Gabrielle et al., 1998). We also expect the proposed structure to be useful for modelling LAI of other arable crops, with particular relevance to those with a long growth cycle. It represents a coherent combination of commonly-used equations for the various processes in leaf area development that have been tested for a range of crops and climates.

Acknowledgements

Technical assistance of M. Lauransot, P. Thiébeau, and E. Caron in the collection of field data, and contribution of F. Vardon to model programming are acknowledged. We also thank an anonymous referee for helpful suggestions on the manuscript. This work was partly supported by the French Agency for Environmental Protection and Energy Control (ADEME), the Centre Technique Interprofessionnel des Oléagineux Métropolitains (CETIOM), and the AIP Ecofon contract (INRA).

References

Amir, J., Sinclair, T.R., 1991. A model of the temperature and solar radiation effects on spring wheat growth and yield. Field Crops Res. 28, 47–58.

Andersen, M.N., Heidman, T., Plauborg, F., 1996. The effects of drought and N on light interception, growth and yield of winter oilseed rape. Acta Agric. Scand. Sect. B Soil Plant Sci. 46, 55–67.

Caron, E., 1995. Etude de la mise en place de l'indice foliaire chez le colza d'hiver avec prise en compte de la contrainte azotée. MSc Thesis, ENSA Toulouse, France.

Cellier, P., Ruget, F., Chartier, M., Bonhomme, R., 1993. Estimating the temperature of a maize apex during early growth stages. Agric. For. Meteor. 63, 35–54.

Derache, P., Guen, H.L., 1986. Valorisations industrielles de la luzerne: modélisation technico-économique. MSc Thesis, ESA Angers, France.

Duru, M., Ducrocq, H., Tirilly, V., 1995. Modelling growth of cocksfoot (*Dactylis glomerata* L.) and tall fescue (*Festuca arundinacea* Schreb.) at the end of spring in relation to herbage N status. J. Plant Nutr. 18, 2033–2047.

Gabrielle, B., 1996. Modélisation des cycles des éléments eau-carbone-azote dans un système sol-plante, et application à l'estimation des bilans environnementaux des grandes cultures. PhD Thesis, Ecole Centrale Paris, France, 112 pp.

Gabrielle, B., Denoroy, P., Gosse, G., Justes, E., Andersen, M.N., 1998. Development, calibration and test of a CERES-type model for winter oilseed rape. Field Crops Res. (this issue).

Gastal, F., Bélanger, G., Lemaire, G., 1992. A model of the leaf extension rate of tall fescue in response to nitrogen and temperature. Ann. Bot. 70, 437–442.

Gosse, G., Rollier, M., Rode, J., Chartier, M., 1983. Vers une modélisation de la production chez le colza de printemps. In: Proceedings of the 6th International Rapeseed Congress, Paris.

Gosse, G., Varlet-Grancher, C., Bonhomme, R., Chartier, M., Allirand, J., Lemaire, G., 1986. Production maximale de matière sèche et rayonnement intercepté par un couvert végétal. Agronomie 6, 47–56.

Greenwood, D.J., Lemaire, G., Gosse, G., Cruz, P., Draycott, A., Neeteson, J.J., 1990. Decline in percentage N of C3 and C4 crops with increasing plant mass. Ann. Bot. 66, 425–436.

Habekotté, B., 1996. Winter oilseed rape: analysis of yield formation and crop type design for higher yield potential. PhD Thesis, Wageningen Agricultural University, Netherlands, 156 pp.

IBSNAT, 1990. Network report 1987–1990. Technical report, Univ. of Hawaï, Honolulu, HI, USA.

Jensen, C., Stougaard, B., Olsen, P., 1994. Simulation of water and N dynamics at three Danish locations by use of the DAISY model. Acta Agric. Scand. Sect. B Soil Plant Sci. 44, 75–83.

Jones, C.A., Kiniry, J.R., 1986. Ceres-N Maize: a simulation model of maize growth and development. Texas A&M Univ. Press, College Station, Temple, TX, 194 pp.

Lemaire, G., Gastal, F., Salette, J., 1989. Analysis of the effect of N nutrition on dry matter yield of a sward by reference to potentiel yield and optimum N content. In: Proc. XVIth Int. Grasslands Congress, Nice, France, pp. 179–180.

Lemaire, G., Onillon, B., Gosse, G., Chartier, M., Allirand, J., 1991. Nitrogen distribution within a lucerne canopy during regrowth: relation with light distribution. Ann. Bot. 68, 483–488.

Leterme, P., 1985. Modélisation de la croissance et de la production des siliques chez le colza d'hiver; application à l'interprétation des résultats de rendements. PhD Thesis, Institut National Agronomique Paris-Grignon, France, 112 pp.

Mendham, N.J., Salisbury, P.A., 1995. Physiology: crop development, growth and yield. In: Kimber, D., McGregor, D.I. (Eds.), Brassica Oilseeds: Production and Utilization. CAB International, Wallingford, UK, pp. 11–64.

Morrison, M.J., Stewart, D.W., McVetty, P.B.E., 1992. Maximum area, expansion rate and duration of summer rape leaves. Can. J. Plant Sci. 72, 117–126.

Muchow, R.C., Sinclair, T.R., Bennett, J.M., 1990. Temperature and solar radiation effects on potential maize yields across locations. Agron. J. 82, 338–343.

Petersen, C.T., Jorgensen, U., Svendsen, H., Hansen, S., Jensen, H.E., Nielsen, N.E., 1995. Parameter assessment for simula-

tion of biomass production and N uptake in winter rapeseed. Eur. J. Agron. 4, 77–89.

Sinclair, T.R., 1994. Limits to crop yield? In: Boote, K.J. et al. (Eds.), Physiology and determination of crop yield. ASA Publ., Madison, WI, pp. 509–532.

Sinclair, T.R., Amir, J., 1992. A model to assess nitrogen limitations on the growth and yield of spring wheat. Field Crops Res. 30, 63–78.

Smith, J.U., Smith, P., Addiscott, T.M., 1996. Quantitative methods to evaluate and compare Soil Organic Matter (SOM) models. In: Powlson, D.S., Smith, P., Smith, J.U. (Eds.), Evaluation of Soil Organic Matter Models. NATO Special Series, Vol. I 38, Springer-Verlag, Berlin, pp. 181–199.

Soontornchainaksaeng, P., Gosse, G., Chartier, M., 1998. Mise au point d'un nouveau sous-model de mise en place de la surface foliaire dans le model CERES-sorghum. Agronomie (in press).

Spitters, C.J.T., van Keulen, H., van Kraalingen, D.W.G., 1989. A simple and universal crop growth simulator: SUCROS87. In: Rabbinge, R., Ward, S., van Laar, H. (Eds.), Simulation and System Management in Crop Protection. Simulation Monograph Vol. 32, Pudoc, Wageningen, Netherlands, pp. 147–181.

Triboi-Blondel, A., 1988. Mise en place et fonctionnement des feuilles de colza d'hiver: relations C–N et sénescence. In: INRA-CETIOM (Ed.), Colza: Physiologie et Élaboration du Rendement, CETIOM edn., Paris, pp. 192–221.

Varlet-Grancher, C., Bonhomme, R., Chartier, M., Artis, P., 1982. Efficience de la conversion de l'énergie solaire par un couvert végétal. Oecol. Plant. 3, 3–26.

Villalobos, F.J., Hall, A.J., Ritchie, J.T., Orgaz, F., 1996. OILCROP-SUN: a development, growth, and yield model of the sunflower crop. Agron. J. 88, 403–415.